Heliyon 7 (2021) e07444

Contents lists available at ScienceDirect

Heliyon

journal homepage: www.cell.com/heliyon

Research article

Porosity and permeability of karst carbonate rocks along an unconformity outcrop: A case study from the Upper Dammam Formation exposure in Kuwait, Arabian Gulf

Fowzia H. Abdullah *

Kuwait University, Faculty of Science, Earth and Environmental Science Department, P.O. Box 5969, Safat, 13060, Kuwait

ARTICLE INFO

Keywords:
Porosity
Permeability
Carbonates
Paleokarst
Dammam
Diagenesis

ABSTRACT

Diagenetic changes are a concern in carbonate petroleum reservoir management. One of the challenges is to determine whether the pore systems are related to diagenesis and/or depositions, and how associated mechanisms affect reservoir quality. The purpose of this study was to assess variations in porosity and permeability due to diagenetic processes in the paleokarst zone of the Middle Eocene Upper Dammam Formation in Kuwait. This zone is 14 m thick and exposed in a quarry in southern Kuwait. The exposed section is divided into three lithological units, described here from the bottom to top: chalky dolostone, karst dolostone, and karst carapace. These rocks have been affected by several diagenetic processes, including dolomitisation, dissolution, cementation, replacement, recrystallisation, and fracturing. Significant variations have been observed in porosity and permeability, both vertically and horizontally. In the chalky dolostone layer, the highest porosity and permeability were measured at 53 % and 6000 mD, respectively. The maximum porosity and permeability in the karst dolostone layer were 44.23 % and 1140 mD, respectively. The karst carapace had the lowest porosity (30 %) and permeability (100 mD). Majority of the porosities were of isolated mouldic or vuggy forms. Pores formed in the rock framework were vuggy, fractured, and more connected. They were formed at later stages by meteoric water dissolution, acidic gases produced during the thermal maturation of kerogen in the petroleum source rocks, or a combination of both processes. The results of this study may be applicable to analogous subsurface carbonate reservoir rocks.

1. Introduction

Reservoirs in carbonate rocks account for approximately 50 % of oil and gas sources worldwide (Mazzallo, 2004). Their mineral compositions are chemically unstable, and their diagenesis has a greater effect on reservoir quality compared to that of sandstone rocks (Murray, 1960; Tucker and Wright, 1990; Mazzallo, 2004). Karstification can occur where rock surfaces are exposed either by uplifting, eustatic sea level changes, or unconformities. Stresses released by uplifting or unloading-associated erosion result in rock fractures and increases in permeability, where meteoric water invades the rock and different diagenetic processes occur, such as dolomitization and processes related to solution porosity (Mazzallo, 2004; Ford and Williams, 2007; Feazel, 2010; Sayago et al., 2012).

Many of the larger Middle Eastern petroleum reservoirs are situated in carbonate reservoirs, where the high quality of their petroleum originates in vugs and karst limestone; examples are the Permian Khuff gas, Dalan-Kangan gas, Mauddud oil, and Mishrif oil reservoirs (Selly, 1998; Dizaji and Bonab, 2009; Mahdi et al., 2013; Leyerer and Meyer, 2010; Lindsay et al., 2010; Yamamoto et al., 2011)).

The exposed karst zone in the Upper Dammam Formation in Kuwait is an excellent example of a complex domain of dissolution, precipitation, and diagenesis in extensively chertified dolostone (Khalaf and Abdullah, 2015). The accessibility of these rocks within the study area (Figure 1) provides an opportunity to assess the magnitude and distribution of these processes within the studied rocks. Such opportunities are not present for subsurface rocks.

The Dammam Formation constitutes the upper layers of the Hasa Group sequence of the Arabian platform and extends across all the Arabian Gulf countries, with a slight increase in thickness towards the east (Lababidi and Hamdan, 1985). It is from Middle to Late Eocene age (Lutetian to Priabonian, 49–33.7 Ma) (Ziegler, 2001). During this time

* Corresponding author.
E-mail address: fozabd2008@gmail.com.

https://doi.org/10.1016/j.heliyon.2021.e07444
Received 22 August 2020; Received in revised form 6 January 2021; Accepted 26 June 2021

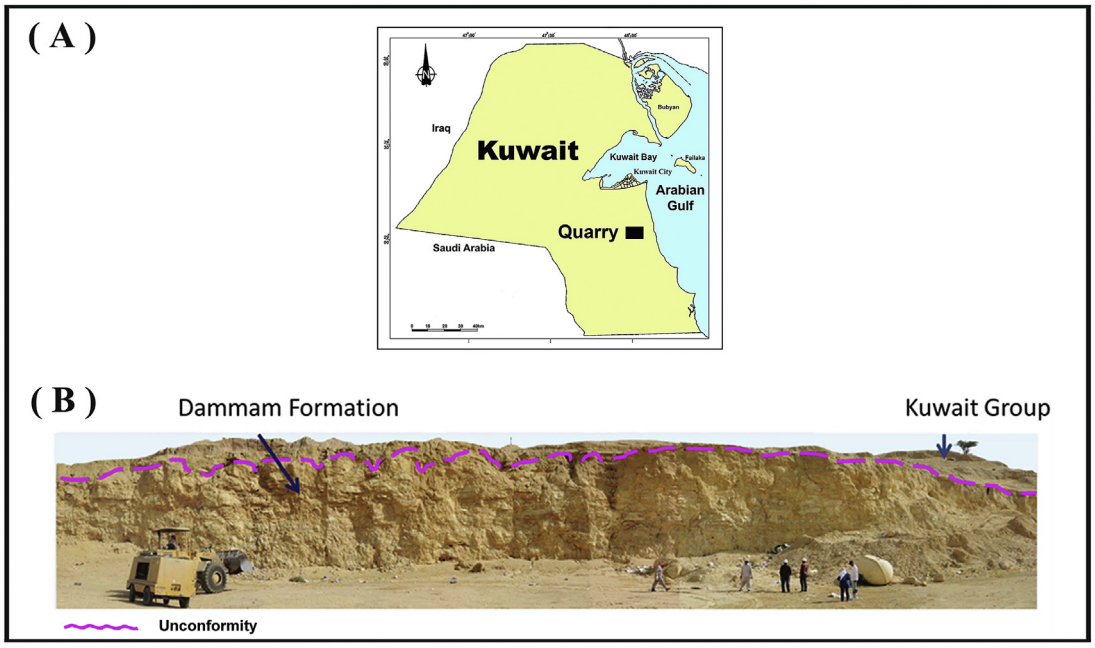

Figure 1. (A) Location map of Ahmadi Quarry; (B) Field photograph of the exposed part of the Dammam formation.

period, the eustatic sea level gradually fell (Haq et al., 1988) where the wide eastern shelf of the Arabian Plate was submerged, and it was subsequently covered by limestone, dolomite, marl, and shale. The base of the Dammam Formation represents an open marine environment, whereas the upper layers indicate a previously shallow marine environment and a siliciclastic influence from the west (Alsharhan and Nairn, 1997; Swart et al., 2005).

In Kuwait, the Dammam Formation is represented by a sequence of limestone and dolomite from the Middle Eocene ages (Lutetian) (Parson Corporation, 1963; Bergstrom and Aten, 1964; Burdon and Al-Sharhan, 1968; Alsharhan and Nairn, 1997). It varies in thickness from 150 m in the southeast to 275 m in the northeast (Al-Awadi et al., 1999; AL-Sulaimi et al., 2004), and is overlain by the Mio-Pleistocene Kuwait Group clastic sequence (Owen and Nasr, 1958). This formation is exposed in a rock quarry located in the southeast of the state of Kuwait, where its upper surface is just a few meters below ground level (Fuchs et al., 1968; Al-Awadi et al., 1999; Khalaf and Abdullah, 2013; 2015). The Dammam Formation, including foraminifera wackestone, packstone, and laminated wackstone, was deposited within a shallow coastal environment, ranging mostly from tidal flats to backshore lagoons. Vertical variations in facies are related to previous fluctuations in sea level. A recent study by Tanoli and Al-Bloushi (2017) on the Dammam Formation was based on rock cores from wells drilled in the Burgan Field, in the eastern section of the Ahmadi quarry. They showed that the formation displayed two transgressive-regressive depositional sequences. The formation that began establishing during periods of sea transgression consisted of muddy limestone and dolomitic limestone deposited in a low-land coastal environment. Frequent flooding facilitated the deposition of black mudstone facies, which was later covered with nummulitic limestone under shallow-water conditions. A second sea transgression period occurred in the middle of the Dammam Formation, and chalky micritic facies were deposited in a quiet lagoon environment. The Zagros orogeny and uplifting at the eastern margin of the Arabian Plate exposed the Dammam Formation throughout the Oligocene period (Mina et al., 1967; Buday, 1980; Beydoun, 1988; Khalaf et al., 1989). The observed karstification processes are associated with these unconformities.

The purpose of this study was to assess the petrophysical properties (porosity and permeability) of the exposed Upper Dammam Formation and to determine their variability within different rock facies. It also discusses the impact of diagenesis on these properties. The results of this study may be applicable to analogous subsurface carbonate reservoir rocks, where the unconformities in carbonate rock surfaces are one of the challenges for petroleum exploration. The study of the exposed rock outcrop also offers an excellent opportunity for use as a model of petroleum exploration in karst limestone along an unconformity.

2. Field occurrence

The Upper Dammam Formation is exposed within a quarry located at the top of the Al Ahmadi ridge, an anticlinal structure, in the southeast of Kuwait (Figure 1). The three main lithological units within this exposed formation are clearly recognisable within various quarry rock cuts, as reported by Khalaf et al. (2018). These are, from bottom to top: (a) bedded chalky dolostone with chert bands; (b) hard karstified dolostone, defined here as karst zone; and (c) hard calcitised and silcretised dolocretic duricrust, denoted here as karst carapace. This sequence is extensively fractured and unconformably overlain by the siliciclastic sequence of the Mio-Pleistocene Kuwait group (Figure 2-A).

The quarry occupies an area of about 4 km^2 and has four main quarrying levels that expose near vertical rock cuts (Figure 2-B). After thorough examination of the exposed rocks within each of these levels, sixteen sites were chosen for detailed investigation and lithological profile construction (Figure 3). The location of these sites is shown on a simplified geologic map of the quarry (Figure 2-B).

Detailed rock descriptions, rock facies, and diagenetic studies on these lithological units were performed by Khalaf et al. (2018) and are summarised below.

2.1. Lithological units

2.1.1. Chalky dolostone unit

The chalky dolostone sequence is well exposed at locations P6, P7, and P8, where it is up to 10 m in thickness (Figure 3). It consists of a thick-bedded white friable porous chalky dolostone. The rock was selectively dissolved during extensive karst episodes, as indicated by an array of karst features (Figure 4-A). These include dolines, pinnacles,

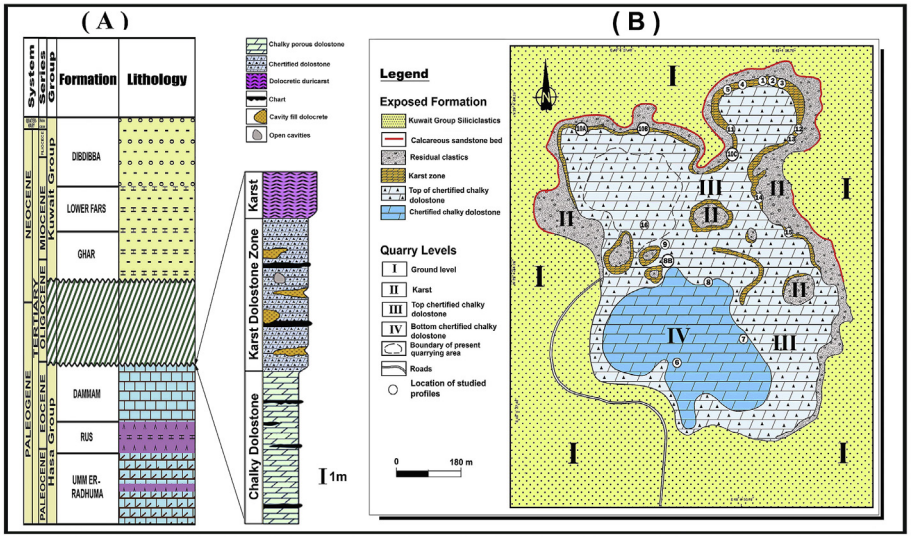

Figure 2. (A) Lithological sequence of the studied Dammam formation; (B) Simplified geological map of the quarry.

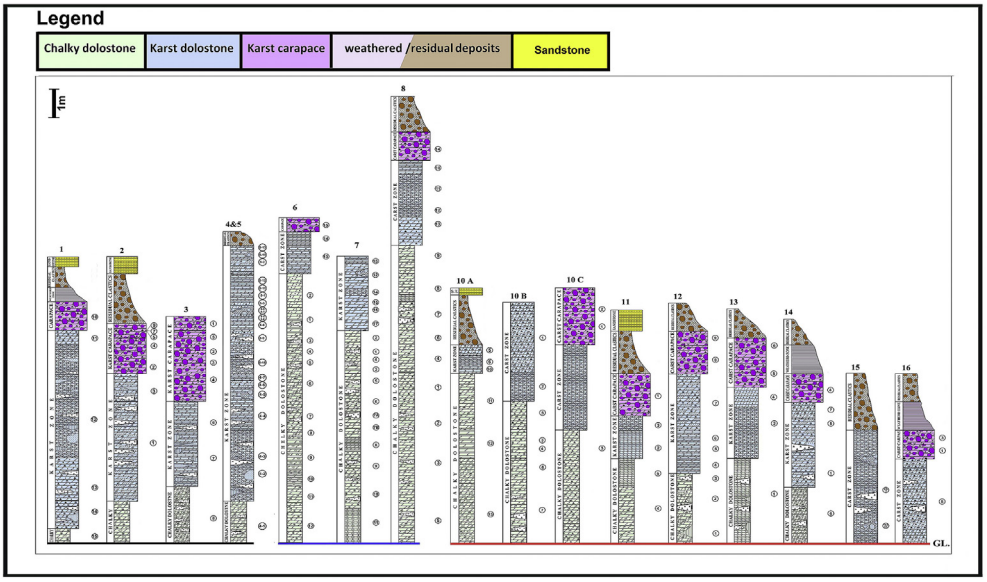

Figure 3. Lithological units in the profiles of the studied sites within the Ahmadi quarry. The weathered/residual deposits and sandstone are layers above the unconformity surface and on top of the studied section. The numbers shown on the right side of each profile are the sample numbers.

solution channels, and caves. Discontinuous chert bands and elongated flat chert nodules are present along the bedding planes and within the chalky dolostone beds. Extensively burrowed chalky dolostone beds occur at several horizons, which are characterised by mottled patterns with dark porous dolomite patches. Large molluscan fossils (moulds and casts) are present in large numbers in the top part of this sequence. The following four main facies are recognised within this chalky dolostone unit:

1) *Dolomitic wackestone facies:* composed of biogenic framework grains floating in dolomitic micrite of either foraminifera (Figure 5A-a) or molluscan shell fragments (Figure 5A-b).
2) *Dolomitic mudstone facies:* burrowed greyish and fractured thin beds within the wackestone facies (Figure 5A-c).
3) *Dolomitic packstone facies:* thin-bedded dolomitic foraminiferal packstone and dolomitic pelletal packstone (Figure 5A-d).
4) *Chertified dolostone facies:* silicified dolostone with moulds (Figure 5A-e).

The allochems within these facies were mostly dissolved, leaving mouldic pores. Most of the foraminiferal tests and ostracods were replaced by dolomite, while their chambers were left open, forming intragranular and mouldic pores. Dolomite is precipitated within the chambers of some foraminifera.

2.1.2. Karst dolostone zone unit

This rock unit is up to 8.5 m thick and differs significantly from that of the underlying chalky dolostone; it is extensively chertified and contains caverns. It is characterised by an abundance of cavity-filled dolocrete (Figure 4A-d &f). Although bedding can be recognised, karstification has significantly disrupted the original bedding. The rocks of this sequence have drastically changed as a result of extensive dolomitization, karstification, and consequent diagenetic alteration. The following four facies are recognised in this unit:

1) *Dolomitic mudstone facies:* This is the most dominant facies. It is hard, whitish to buff coloured, vuggy (μm to mm size), cracked, and mostly

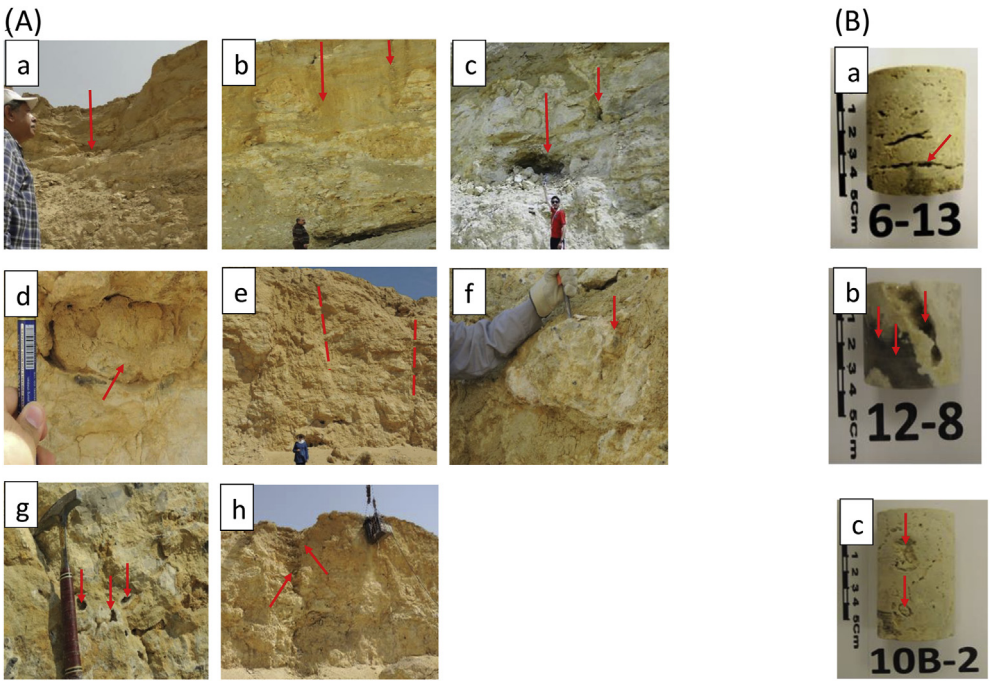

Figure 4. (A) Field photos showing the various sizes of the karst features and porosities; a-doline; b-pinnacles; c-cave; d-dolocrete nodule; e-fracture; f-large dolocrete nodule within cavity filled by siliciclastic deposits; g-geodes with calcite crystals, h-channels shaped by leaching along fractures. (B) Type of macroporosities a-vuggy, b-vuggy and intercrystalline, c-mouldic.

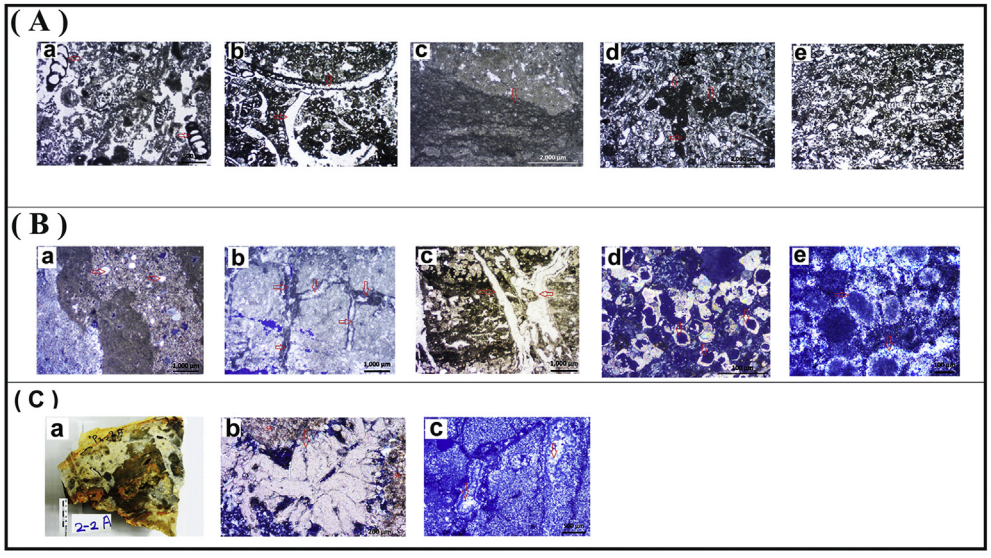

Figure 5. Photomicrographs of the various facies of the Dammam Formation. (A) Chalky dolostones: a-dolomitic foraminiferal wackestone (arrows show forams); b-dolomitic molluscan wackestone (arrows show mollusc grains); c-dolomitic mudstone algal mat (arrow); d-dolomitic pelletal packstone; e-chertified dolostone. (B) Karst dolostone zone: a-dolomitic mudstone, with an arrow pointing towards dolomite grains; b-shrinkage cracks (arrows) in the dolomitic mudstone; c-root burrows (arrows) in dolomitic mudstone; d-vugs filled with hollow dolomite rhombs (arrows) in the dolomitic mudstone; e-silicified dolomitic grainstone, with an arrow showing the cement between the grains. (C) Karst carapace: a-slabbed hand specimen of the karst carapace rocks; b-calcitised dolocrete cemented (arrows) by sparry calcite SP; c-silicified calcrete, with the arrows showing the calcite crystals.

chertified with abundant cavity-filled dolocrete (Figure 5B-a). Vertical and horizontal shrinkage cracks (Figure 5B-b), root burrows of 0.5 cm diameter (Figure 5-B-c), and vugs filled with hollow dolomite rhombs mixed with gypsum and alunite (Figure 5B-d) were also observed.

2) *Dolomitic wackestone facies:* This is the second-most dominant facies; it is vuggy and fractured. Abundant bivalve moulds (up to 2 cm long) clustered horizontally in thin bands were common.
3) *Dolomitic packstone facies:* This is very limited, vuggy dolostone containing abundant and poorly sorted allochems (80 %) mixed with carbonate mud. Chertification was developed by the precipitation of various types of quartz in the pores and vugs.
4) *Dolomitic grainstone facies:* Occurs only in profile 5. The rock is almost completely silicified, leaving the original texture of the dolomitic grainstone as impressions. It comprises allochem grains and pellets, with their original grain impressions, which are replaced by microquartz, while the interpelletal pores are cemented with coarser quartz crystals (Figure 5B-e).

2.1.3. Karst carapace unit

This occurs at the topmost part of the karst dolostone sequence at some sites, as a very hard crust formed of extensively calcitised, silicified, and gypcretised dolocrete. It varies in thickness between 0.50 m and 2.70 m. Rocks of this unit display a composite pattern, with patches of cavity-filled dolocrete and remnants of dolostone host compartments (Figure 5C-a). Two generations of dolocrete were recognised, namely, a light-coloured immature dolocrete that encloses a

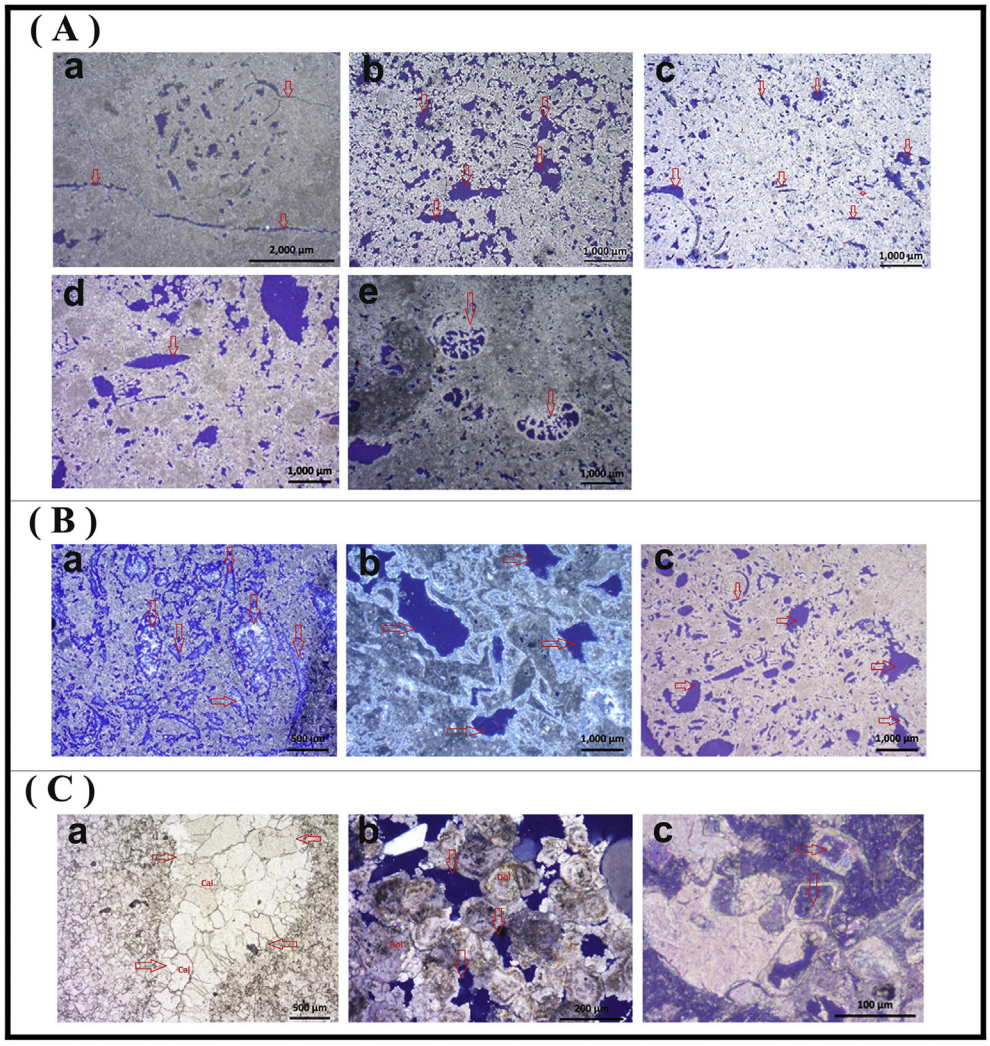

Figure 6. Photomicrographs illustrating the types of porosities (arrows) within various rock facies. (A) Chalky dolostone; a: fracture porosity; b: vug porosity; c: mouldic porosity; d: moulds of gypsum crystals; e: intragranular porosity within foraminifera; (B) Karst dolostone zone; a-ghost porosity; b-isolated scattered partially cemented pores (moulds and cavities); c-porous karst dolostone. (C) Karst carapace; a-pores are cemented with calcite Cal; b-isolated pores between the dolomite particles; c-intracrystalline pores within dissolved dolomite crystals.

dark-coloured mature dolocrete. Cavity-filled dolocrete may occur as coalesced nodules. This unit has abundant occurrences of geodes that vary in size from a few millimetres to several centimetres (Figure 4A-g). These geodes are partly or completely cemented by calcite, and a few are cemented by quartz. Some vugs and fractures are cemented with calcite (Figure 5C-b) and gypsum. Some patches have been completely silicified (Figure 5C-c).

These diagenetic processes are explained in detail by Khalaf et al. (2018).

3. Material and methods

3.1. Sampling

A total of 134 rock and sediment samples representing various rock types were collected.

Rock slabs from each rock sample were prepared for visual examination, standardised for thickness. Lithostratigraphic sections were obtained for each rock unit, following the method by Khalaf et al. (2018). The profiles are shown for each unit (Figure 3).

3.2. Porosity and permeability measurements

Investigations of large pores, more than 5 cm in diameter, were carried out visually in the field. Their size and distribution were measured and calculated. A total of 150 core plugs were drilled, parallel and vertical to the bedding plane, and collected from each lithological unit, for porosity and permeability measurements. The core plugs were washed and, to remove humidity, dried in an oven at temperatures under 40 °C until their weights were stable. The total porosity of each core plug was measured using a helium porosimeter PHI-220. The permeability of the core plugs was measured using a gas Permeameter-KA-210 instrument.

In addition to conventional porosity measurements, a thin-section petrograph image analysis technique was applied. Photographs of 56 thin sections were taken under plane- and cross-polarised light using a digital camera attached to a petrographic microscope, to quantify and qualify the porosity. Image analysis was conducted using analySIS (Olympus Soft Imaging Solutions). To ensure inclusion of the largest estimated porosities, calculations were carried out by averaging the calculated porosity of three microscopic views of each thin section.

4. Results

4.1. Visual assessment of porosity

Different porosities were observed in the studied samples. The observed categories are numbered and described below:

1 Porosity was not observable in rock specimens or thin sections and was mostly represented by major open fractures and large cavities (Figure 4A-c, d, e (diameter magnitudes greater than decimetres).

Table 1. Image porosity, plug porosity, and permeability in the three rock units in the 16 studied rock profiles.

Rock Unit	Type Of Analysis		Profile No 1	2	3	4 & 5	6	7	8	10A	10B	10C	11	12	13	14	15	16	Average
Chalky Dolostone	Image Porosity %	Range	6.11-11.79				0.06-51.22	0-14.49	7.44-13.33	3.05-9.92	0.18-23.71	5.98	9.29	0-13.98	12.00	18.21			
		Average	8.95				24.2	8.45	8.33	6.34	12.6	5.98	9.29	7.78	12.00	18.21			**11.10**
		Type	Vuggy				Vuggy & Mouldic	Vuggy & Mouldic	Vuggy & Mouldic	Vuggy & Mouldic	Vuggy & Mouldic	Vuggy	Vuggy & Mouldic	Vuggy & Mouldic	Vuggy	Vuggy			
	Plug Porosity %	Range	6.66-25.10		34.10-34.67	19.26-19.29	0.57-53.74	0.17-59.58	0.46-38.36	12.91-34.25	12.31-44.68	19.05	10.88	3.21-37.77	21.21	41.24			
		Average	15.73		35.88	19.27	27.7	26.32	23.95	24.58	35.82	19.05	10.88	22.28	21.21	41.24			**24.92**
	Permeability mD	Range	2.86-855.28		564.93-653.15	3.61-569.88	3.29-3053.88	1.44-2311.89	4.11-6051.30	5.57-786.67	191.62-3492.83	174.97	173.20	2.90-1662.32	1488.60	5759.25	97.97-2692.21	103.23	
		Average	233.77		609.04	286.74	780.18	588.31	1545.42	444.92	2333.09	174.97	173.20	916.60	1488.60	5759.25	1073.18	103.23	**1100.70**
Karst Zone	Image Porosity %	Range	5.43-15.98	1.33-7.3		0.01-27.55	5.21-9.74	0-36.47	4.95-14.77	0-4.53	0.00-4.00		3.49-9.69	7.23-14.73	9.35-16.14	5.29-17.55	0-13.02	1.21	
		Average	10.02	4.8		10.22	7.35	12.55	9.83	1.54	2.00		6.57	12.58	12.75	11.42	5.037	1.21	**8.30**
		Type	Vuggy & Moldic	Vuggy		Vuggy & rare Interparticle and Interparticle	Vuggy & Mouldic	Vuggy & Mouldic	Vuggy	Vuggy	Vuggy		Vuggy	Vuggy & Mouldic	Vuggy	Vuggy	Vuggy & Mouldic	Vuggy	
	Plug Porosity %	Range	3.44-22.78	2.24-7.33	14.47-25.62	1.01-16.64	13.02-25.80	18.33-40.3	6.88-15.94	11.53-15.05	25.52-13.65		6.83-10.75	11.88-20.63	5.53-5.93	6.04-9.20	19.087-44.23	17.48	
		Average	11.56	5.41	20.04	6.45	19.41	29.23	10.86	13.30	19.59		8.79	15.48	5.73	7.62	28.57	17.48	**14.63**
	Permeability mD	Range	3.70-1139.68	0.14-3.47	1.06-2.01	0.39-4.94	3.90-5.38	20.56-867.83	2.38-31.20	1.32-21.96	3.25-121.63		2.51-6.78	3.89-775.79	2.78-4.65	3.85-5.47			
		Average	288.33	1.74	1.53	2.94	4.64	352.22	11.75	9.13	62.44		4.65	286.68	3.71	4.66			**79.57**
Karst Carapace	Image Porosity %	Range	3.4-4.4	0.23	0.07-15.38		1.69-16.6		0.63			1.08-3.11	0	0.00-6.4	0.00-15.29	1.18		0.34-1.32	
		Average	5.55	0.23	6.65		8.12		0.63			2.10	0	3.20	7.65	1.18		0.83	**3.29**
		Type	Vuggy & interparticle	Interparticle	Vuggy		Vuggy & Mouldic & Interparticle		Vuggy			Vuggy		Vuggy	Mouldic & Vuggy	Vuggy		Vuggy	
	Plug Porosity %	Range	4.77	2.26-30.55	4.41-39.23				0.99			8.41-10.49	15.29	8.28-18.86	17.30-23.48	12.41		9.11-23.13	
		Average	4.77	11.76	15.63				0.99			18.9	15.29	13.57	20.39	12.41		16.12	**12.98**
	Permeability mD	Range	68.73	0.63-139.81	0.10-3.65				3.68			1.89-2.18	3.64	2.04-9.05	2.56-4.94	5.93		2.07-5.57	
		Average	68.73	26.44	8.16				3.68			2.04	3.64	5.54	3.75	5.93		3.82	**13.17**

This type of porosity is common in karst dolostone units. Cavities and fractures were sometimes filled with gravel, sand, and silt grains. Water played a role in forming channel shapes, by leaching the rock surrounding these fractures (Figure 4A-h). Most of the fractures were vertical, with rare horizontal orientations. A simulation of the fractures was performed to obtain an appropriate measure of fracture porosity. The simulations were based on fracture distributions that had been measured in the field and with the aid of the field photos. The fracture aperture width was estimated to be approximately 2 mm, and the maximum aperture was approximately 5 mm. The average visual field estimation of the total porosity was approximately 0.60 %, with a maximum fracture porosity of 2 % in highly fractured areas.

2 Porosities with magnitudes in centimetres were mostly represented by the following types: solution vugs, moulds, channels, and fractures that could be seen in rock hand specimens and plugs (Figure 4B).

3 Porosity which was only recognisable in the thin sections and was mostly represented by the following types: fracture, mouldic, vuggy, interparticle, intraparticle, intercrystalline, and intracrystalline.

4.2. Types of porosity in the rock units

4.2.1. Porosity of the chalky dolostone unit

The exposed sequence of this rock unit was extensively fractured. These were tectonic fractures, most of them vertically orientated. These fractures were slightly enlarged by dissolution, and few narrow dissolution channels were recognisable (Figure 4A-h). They provide avenues for water infiltration. Small cavities, which were up to approximately 1 m long and 30 cm high, commonly occurred at the top of the chert bands and might indicate active dissolution of the chalky dolomicrite by the water accumulated at the top of these bands. Such fractures and cavity porosities were quantitatively estimated during drilling operations by reservoir engineering calculations. They can also be observed in image logs (Aghli et al., 2016).

Visual examination of the rock slabs indicated that the chalky dolomicrite rocks are generally porous. Porosity is represented by megapores (>0.2 cm) of dissolution vugs, burrow holes, and mouldic cavities of large gastropods and bivalves. These pores varied in size, between fractions of a centimetre and greater than a centimetre. The visual estimation of this mega porosity ranged between 15.00 and 25.00 %. The estimation was carried out by measuring the total size of the megapores and dividing them over the total area of the slab rock.

Seven types of porosities were recognised in the thin sections: fracture, mouldic, vuggy, interparticle, intraparticle, intercrystalline, and intracrystalline. Fracture porosity was commonly represented by open fractures with an average gap width of a millimetre (Figure 6A-a). This type of porosity constituted <7 % of the total observed porosity. The vug porosity was the most abundant type of porosity in the chalky dolomicrite rocks (Figure 6A-b). They ranged in size between <0.5 mm and >1.5 mm and had an average frequency of 23 % (of the total rock porosity). Mouldic porosity was the second most common type of porosity (Figure 6A-c). Moulds of gypsum crystals were also common in the mudstone facies of the chalky dolostone, as shown in Figure (6A-d). The average frequency of the mouldic porosity was approximately 59 % of the total porosity. Intragranular porosity was also frequently observed and was represented by pores within various types of foraminifera (Figure 6A-e). Intercrystalline and intracrystalline porosities between and within the dolomite crystals, respectively, were also found in this rock unit.

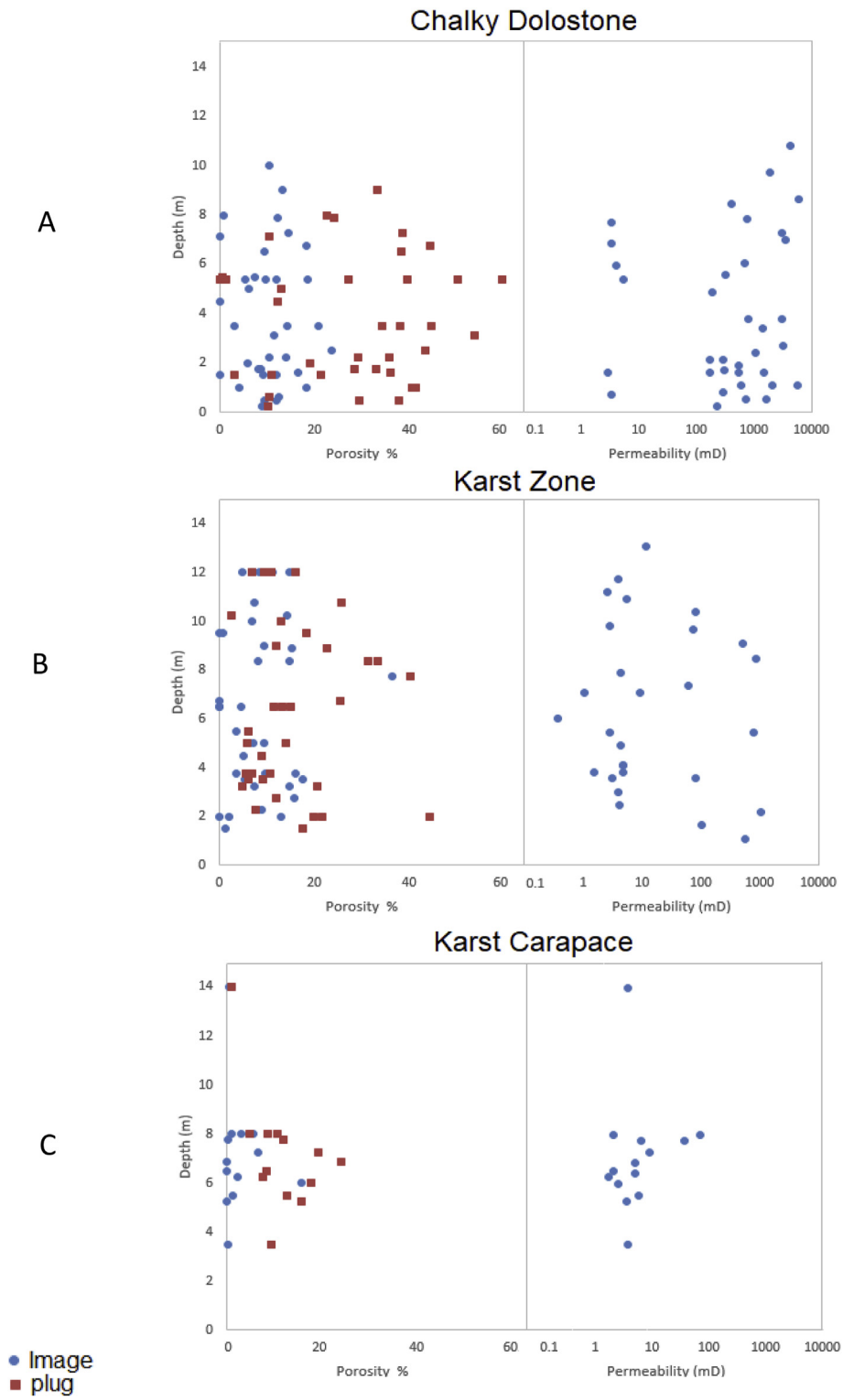

Figure 7. Variation of image and plug porosities and permeability with depth for the chalky dolostone (A), karst dolostone (B) and karst carapace (C) units.

4.2.2. *Porosity of the karst dolostone zone unit*

The pore types in this unit were observed to be similar to those of the chalky dolostone unit, but with more dissolution vugs and cavities. The extensive and intensive calcitisation and silcretisation of the karst dolostones had occluded most of the pore spaces and also occurred as blocked porosities (Figure 6B-a). The remaining porosity was represented by isolated scattered uncemented or partially cemented pores (moulds and vugs) within the calcified and/or silicified parts of the rock (Figure 6B-b). However, some thin beds that had not been affected by diagenesis were still porous (Figure 6B-c). These rocks appeared very porous, but most of the pores were not visibly connected. The mouldic and vuggy porosities constituted approximately 30 % and 45 % of the total porosity, respectively.

4.2.3. *Porosity in the karst carapace unit*

The porosity in this unit was sparse, with most of the pores cemented (Figure 6C-a). Some isolated pores of the intercrystalline type were visible

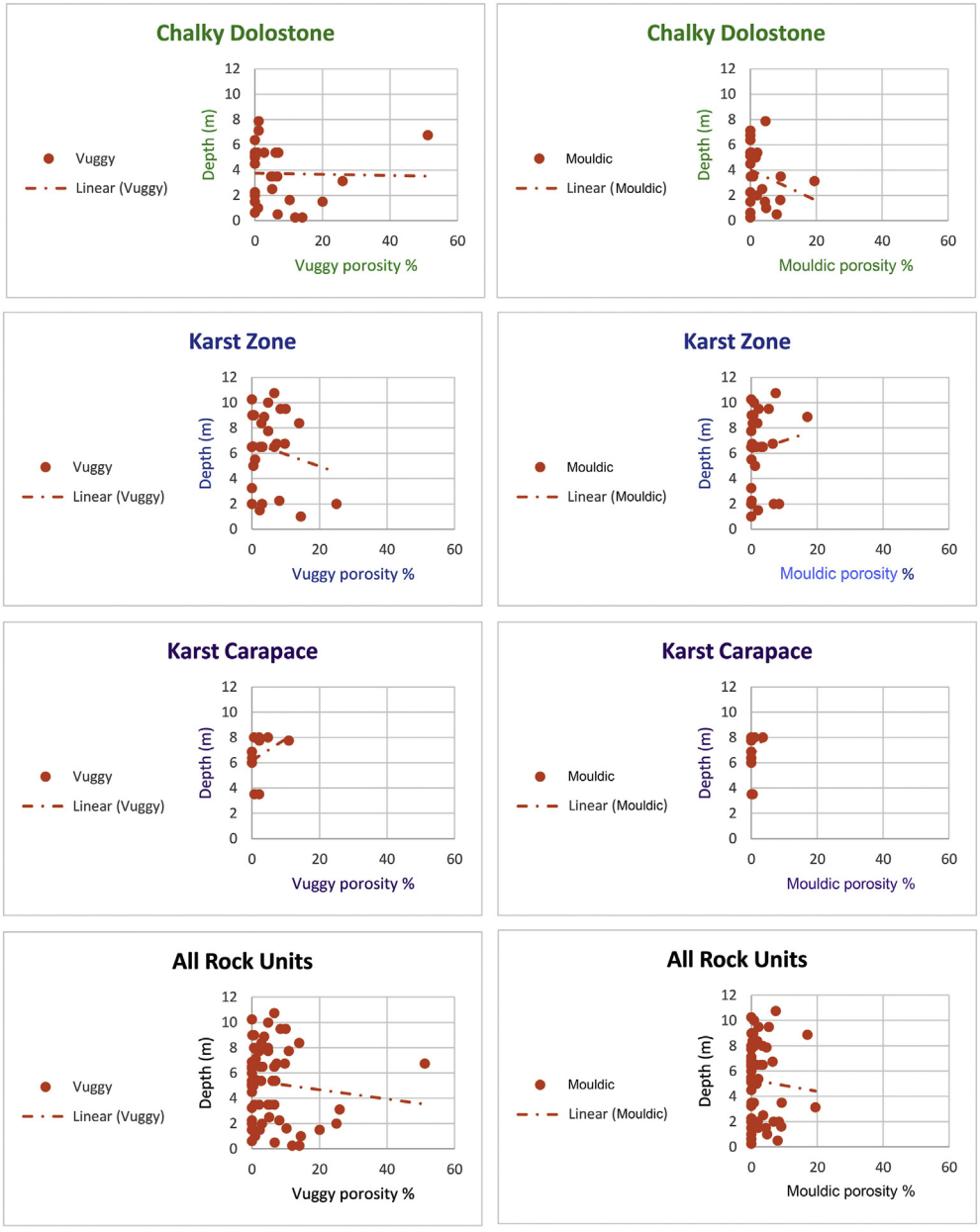

Figure 8. Variations with depth in vuggy and mouldic porosity using image porosity assessments for the three rock units. The top line is for the chalky dolostone, the second line for the karst zone, the third line for the karst carapace and the last line for all the rock units together.

between the dolomite crystals (Figure 6C-b). In this rock unit, intracrystalline porosity was rarely observed within dissolved dolomite crystals (Figure 6C-c).

4.3. Porosity assessment and measurement

4.3.1. Assessments by image processing

4.3.1.1. Variation of pore type with lithology. The results for the profile of each rock unit are listed in Table 1. The dominant porosity type in all rock units was vuggy porosity, and its maximum measured value (51.22 %) was found in the chalky dolostone unit. Minor porosity types observed were interparticle, intercrystalline, and fractured types, and were found in all three rock units.

Average measured porosity in the three rock units ranged from 3.29 to 11.10 %, where the highest porosity was found in the chalky dolostone unit and the minimum in the karst carapace unit.

The highest vuggy porosity variation was found in the chalky dolostone (0.10–51.22 %), while it ranged between 0.20–25 % and 0–15.29 % in the Karst zone and karst carapace units, respectively. A similar pattern was observed for the mouldic porosity, where the highest variation (0.20–19.46 %) was found in the chalky dolostone and the minimum variation (0.10–3.30 %) was found in the karst carapace.

The highest interparticle porosity (7.40 %) and other minor porosity types, such as intercrystalline (1.40 %) and fracture (2.10 %), were found in the karst zone unit.

The large variations in the image porosity values in some samples reflect high heterogeneity in the three rock units. The maximum porosity values in the three rock units were not in the same rock profile; in the chalky dolostone unit and the karst carapace, it was found in profile 6, whereas for the karst zone, it was found in profile 7 (Table 1).

4.3.1.2. Variation with depth. In general, no clear variations or correlations with depth were found in the imaged porosities of the three rock units (Figure 7). However, there was a slight increase in the porosity of the chalky dolostone unit with depth. A depth of zero in the graphs

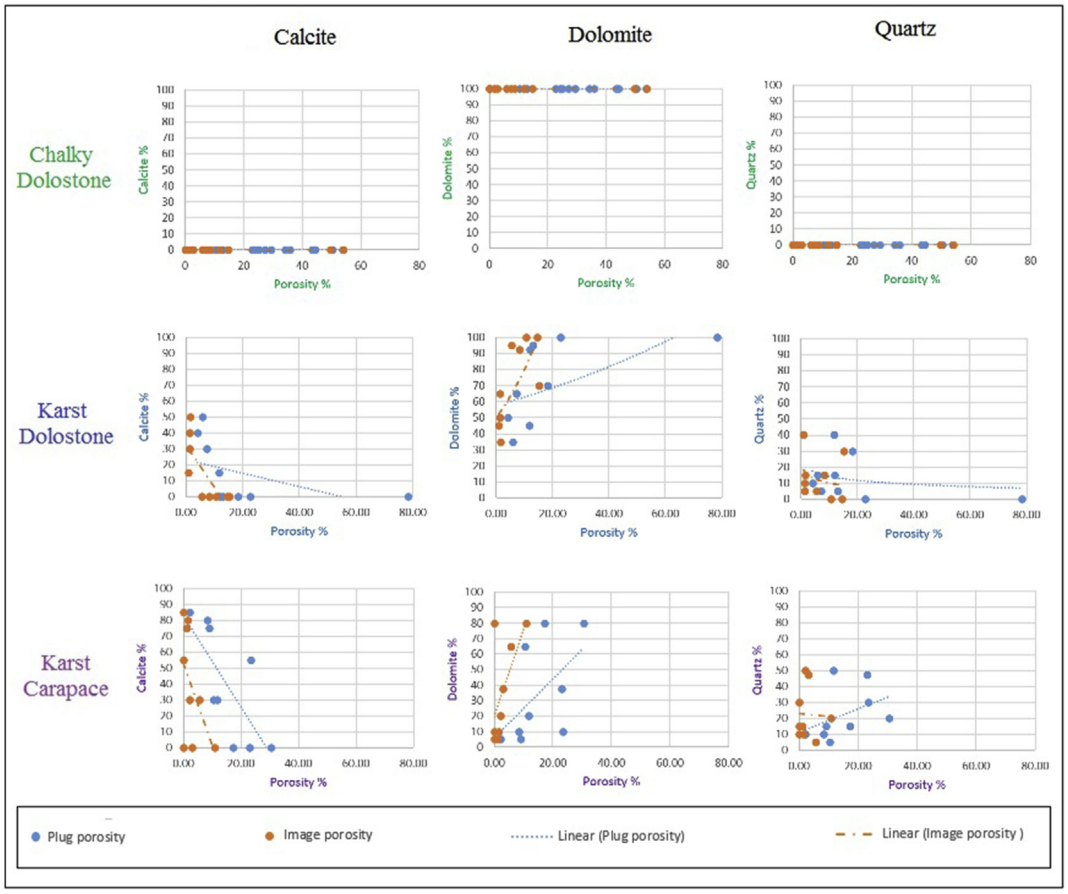

Figure 9. Variations of image and plug porosities with mineral composition, calcite, dolomite and quartz. The upper line shows these variations for the chalky dolostone, the middle line for the karst dolostone and the bottom line for the karst carapace.

Table 2. Summary of porosity and permeability for the rock units and their dominant porosity types.

Rock Unit	Plug Porosity Range %	Image Porosity Range %	Permeability Range mD	Type of porosity
Chalky Dolostone	0.23–53.00	0–24.00	2.90–6051.00	Vuggy (dominant) and Mouldic
Karst Zone	1.00–44.00	0–36.00	1.00–1140.00	Vuggy (dominant), Mouldic, Inter-particle, Intra-particle
Karst Carapace	2.00–39.00	0–15.00	0.10–140.00	Vuggy, Inter-particle

denotes the ground surface level, and the other depth values represent the elevation increasing above ground level.

Vuggy and mouldic porosities tended to become more abundant with increasing depth and lower elevation in the chalky dolostone, and this was a consistent observation, except for one sample at depth 6.75 m, in which the porosity was approximately 50 %. In the karst zone unit, the vuggy porosity increased slightly with depth, while the mouldic porosity showed no clear trend with depth. The karst carapace showed a slight decrease in porosity with depth for both the vuggy and mouldic porosities in the upper two metres (6–8 m) (Figure 8).

4.3.1.3. Variation with mineralogy. The variations in porosities corresponding to mineral composition are shown in Figure 9. This analysis was not applicable to the chalky dolostone unit because the rock was composed only of dolomite. The imaged porosity for both the karst dolostone and karst carapace units showed positive correlations with dolomite concentrations and negative correlations with calcite concentrations. At calcite concentrations of more than 20 % in the karst dolostone, the image porosity dropped to almost zero. In the karst carapace, the rock lost its image porosity at calcite concentrations higher than 60 %. The effect of quartz on the image porosity was not clearly correlated in the karst carapace and karst dolostone units.

4.3.2. Porosity and permeability plug measurements

4.3.2.1. Variation with lithology. The maximum measured average plug porosity (24.92 %) and permeability (1100.70 mD) were found in the chalky dolostone, and the minimum average porosity (13.17 %) and permeability (13.17 mD) were found in the karst carapace unit. The maximum and minimum plug porosity and permeability values in the three rock units were not found in the same profile. For the chalky dolostone unit, the minimum porosity (0.17 %) was found in profile 7, and the minimum permeability (3.20 mD) was found in profile 6, while the maximum porosity (59.60 %) was found in profile 7, and the maximum permeability (6051.30 mD) was found in profile 8 (Table 1). There were also similar variations in the other rock units (Table 1). These

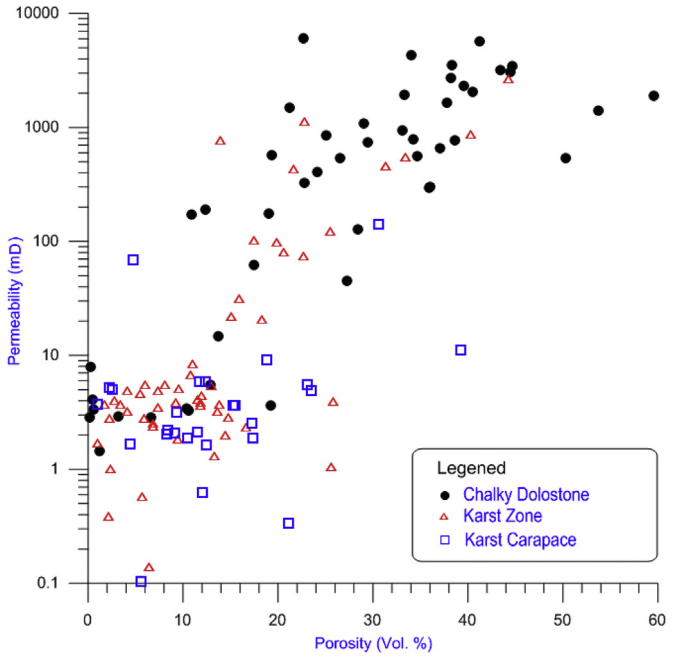

Figure 10. Scatter plot of porosity versus permeability The three circles show the variation between the original rock types and present-day porosity and permeability (compiled from Hartmann and Beaumont, 1999, reprinted with permission from AAPG, whose permission is required for further use).

results, as well as the image porosity results above, indicate that porosity and permeability are not related to the location of the rock unit but rather to other factors, which will be discussed in the subsequent sections.

4.3.2.2. Variation with depth. The three rock units showed large porosity and permeability variations with depth (Figure 7), but there was no clear trend in the variation. The plug porosity and permeability varied at the same depth at certain intervals in the three rock units. At a depth of 5.4 m in the chalky dolostone, the porosity varied between 0.17–59.60 %. The permeability at 2 m depth ranged between 175–296 mD. At a depth of 12 m in the karst dolostone zone, the porosity varied between 6.8–16 %. The permeability at depths of 3.2 m ranged between 3.1–80.3 mD. At a depth of 8 m in the karst carapace units, the porosity ranged from 4.8–10.5 %, while the permeability at the same depth ranged between 2–68 mD.

4.3.2.3. Variation with mineralogy. The variations in the mineral composition and plug porosity for each rock unit are shown in Figure 9. The chalky dolostone unit was composed purely of dolomite. At 100 % dolomite concentration, the porosity showed different values. In contrast, the porosity in both the karst dolostone and karst carapace units increased with dolomite concentration.

The porosity of both the karst dolostone zone and karst carapace units were negatively correlated to calcite. There were many geodes in the karst carapace unit, and some of these geodes were completely cemented with calcite crystals.

The quartz concentration showed a very slight negative effect in the karst dolostone zone but a positive effect in the karst carapace units. The karst zone had bands of chert nodules and field size caverns, which were larger than those measured in the plugs. Quartz and silica had cemented all the vugs, moulds, or any dissolved parts of the precursor dolomite rock. The karst carapace unit showed less clear positive correlations. Quartz in this zone were found in some of the geodes and the silcrete that had replaced the calcite with different forms of quartz.

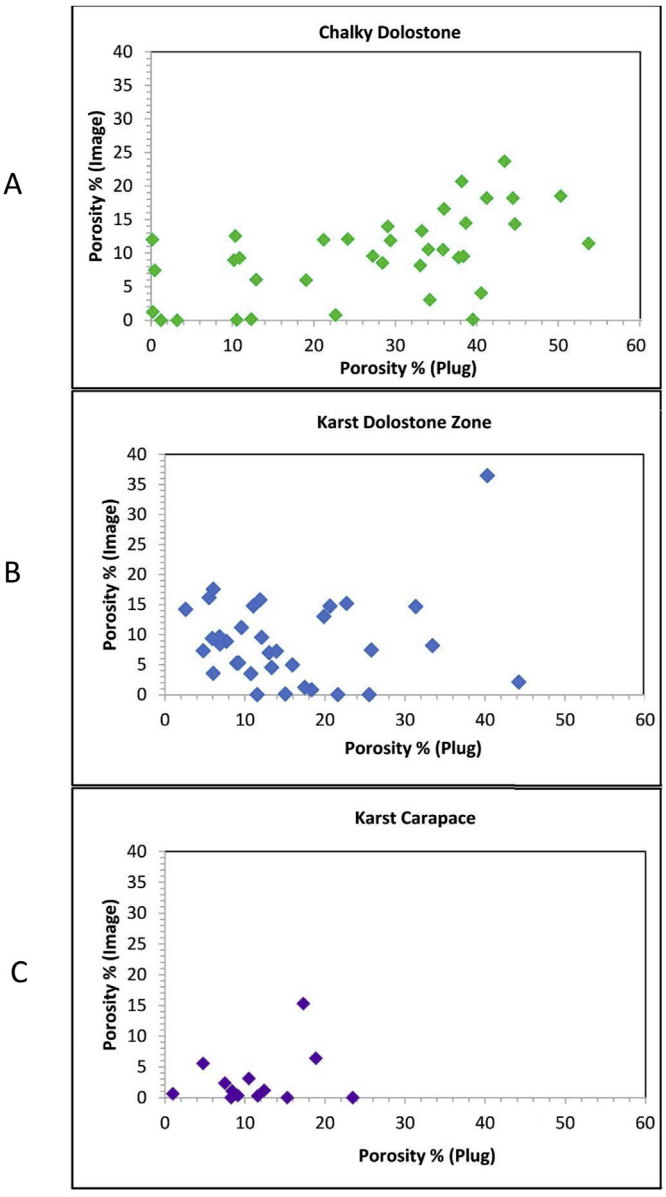

Figure 11. Scatter plot of image and plug porosity for the three rock units. A-chalky dolostone, B- karst dolostone, C- karst carapace.

5. Discussion

The complicated history of diagenesis (dissolution and precipitation, crystallisation, and cementation) in the upper Dammam Formation has caused heterogeneity in the rock characteristics, which is reflected in its porosity and permeability. The variations in porosity and permeability exist both in horizontal and vertical orientations, creating complex heterogeneity in the rock properties, and making composition predictions challenging.

The highest porosity value was found in the chalky dolostone, while the lowest was in the karst carapace unit. All the rock units showed high variations in porosity, which was most obvious in the chalky dolostone and karst dolostone zone units (Table 2). The rocks are dominated by vuggy and mouldic porosity types, which result from dissolution at different periods of diagenesis. There are minor original syndepositional interparticle and diagenetic intercrystalline porosities. Large field-sized

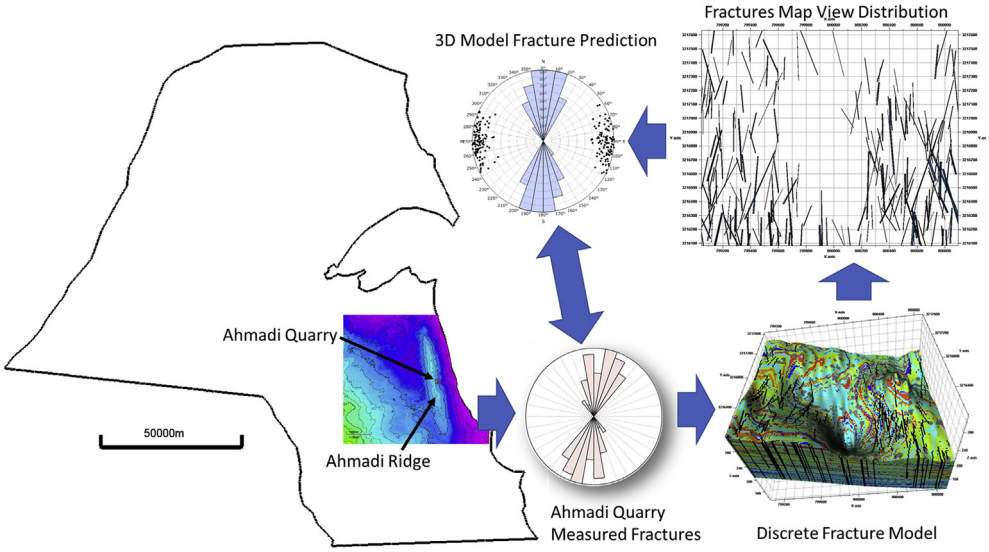

Figure 12. Fracture strikes, dips, and spacing measurements over the Ahmadi Quarry, showed the general N–S to NNE-SSW trend of fractures over the quarry area.

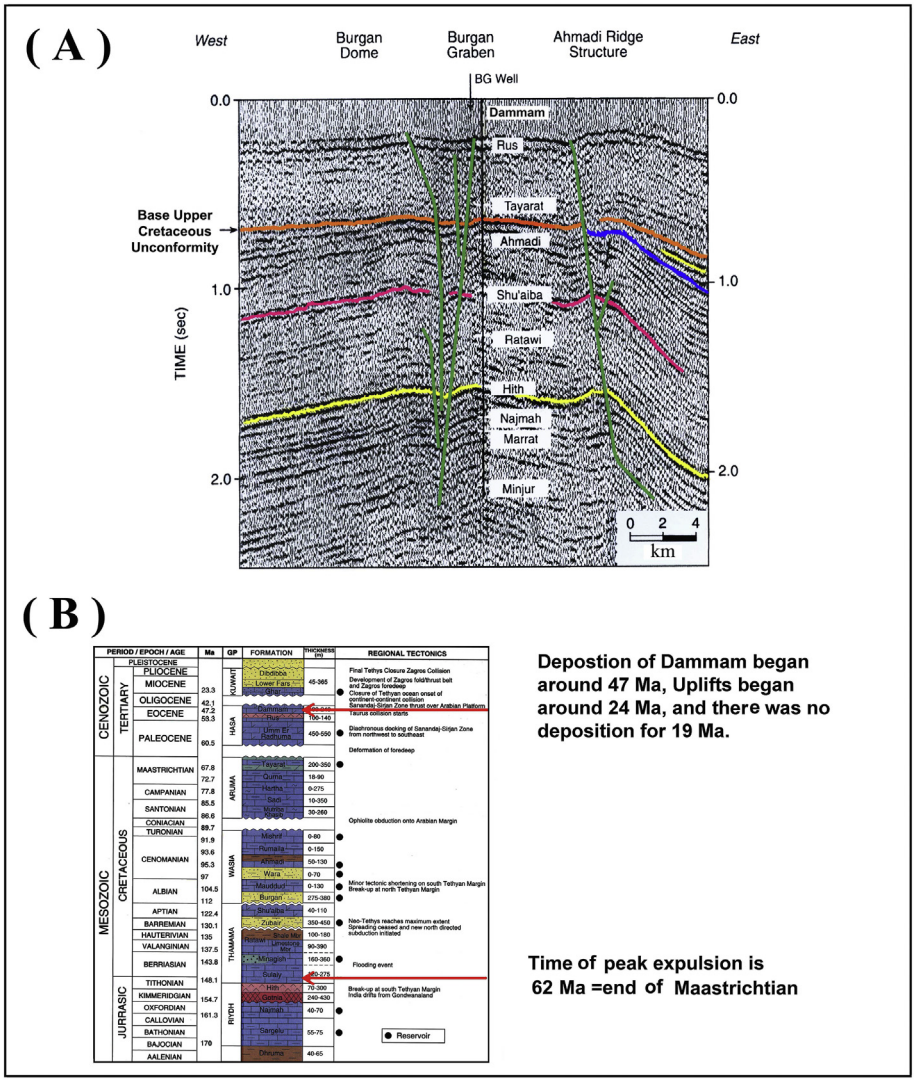

Figure 13. (A) Seismic section on top of Burgan and Ahmadi oil fields showing the faults (Carman, 1996, by permission from GeoArabia), which is one of the paths of gas seepage. (B) Kuwait stratigraphy and oil/gas expulsion time from the source rock (compiled from Abdullah et al., 1997; by permission from GeoArabia).

pores were cavernous and of the fractured type (Figure 4), as large as 3 m wide for the caves and 3 m long for the fractures.

Statistical analysis for all rock units (Figure 10) showed a positive correlation between porosity and permeability. The results show that the chalky dolostone unit exhibits the highest values of porosity and permeability. This was followed by the karst dolostone zone and then the karst carapace unit.

In general, the highest values for both the image and plug porosities and permeabilities were found in the deepest parts of the studied sections, for both the chalky dolostone and karst dolostone units. However, there was no clear trend in the variations with depth for either parameter in the three rock units (Figure 7).

Considering the nature of the original rock, packstone, wackestone, and mudstone, most of these rocks had an average initial porosity of 45 % (Hartmann and Beaumont, 1999). In the study area, the rock material was deposited in a tidal flat and backshore lagoonal carbonate environment (Khalaf et al., 2018). As a result of the diagenetic processes, these rocks (in relation to their quality as a resource reservoir) exhibit reduced porosity values, except for mudstone (Figure 10). However, permeability was enhanced by diagenesis, especially in the chalky dolostone and karst dolostone zone rock units. Poros et al. (2010) found that the porosity of dolostone below unconformities was enhanced by powderization, which might be one of the factors contributing to the increased porosity in the chalky dolostone unit.

Dolomitization may enhance or eliminate rock porosity. The process of dolomitization may occur either by processes replacing original carbonates or by precipitation and filling of the pores with dolomite cement. Replacement of mud-sized grains generally enhances permeability, which can be observed in the karst dolostone and karst carapace units (Figure 9), but this is not the case if dolomitization continued and cemented the pores. This process is termed "overdolomitization" (Yamamoto et al., 2011). In this study, the Dammam Formation had been almost fully dolomitized. Most of the pores were greatly cemented with dolomite, most obviously in the chalky dolomite. In general, tidal flat reservoirs are correlated with diagenetically enhanced porosities, rather than depositional porosities. There is increased dissolution in rocks with higher surface area per volume, which has resulted in the formation of vugs and mouldic porosities. This occurred at the surface and within the carbonate rock, where fluid had flowed through the matrix pores and fractures. As a result, these pores have stabilised and become less soluble by neomorphism (Schlanger, 2005).

The slightly negative correlations between porosity and calcite in both the karst zone and karst carapace units are a result of cementation and calcitisation that occurred during the semi-arid periods at two stages (Khalaf et al., 2018). The geodes, which are larger than the plugs used for the porosity study, are completely cemented with calcite crystals and contributed to even clearer negative correlations with porosity.

The slightly positive correlations of quartz with plug porosity in the karst carapace unit is likely related to the replacement of calcite by quartz, causing some calcite dissolution and an increase in porosity.

The thin-section image used in porosity measurements indicated lower values in relation to plug porosity. This was observed in all three rock units (Figure 7). Some high plug porosities had an image porosity of zero (Figure 11).

The correlations between the image and plug porosities for the three rock units (Figure 11) showed no clear correlations, and the differences between the average image and plug porosities in the rock profiles did not show any clear trend (Table 1). The heterogeneity of these rock units makes it difficult to make horizontally and vertically oriented predictions of their porosities. The imaged porosities did not reflect the total porosity measured by the plugs in these rock units. The porosity of the plugs is shown in the rock framework and is of mainly diagenetic origin, and predominantly related to leaching and fracturing. The size of these pores is much larger than can be measured at microscopic scales, and in fact larger than can be measured using plugs. Examples are the cavernous sizes shown in Figure 4. Fracture strikes, dips, and spacing measurements have been performed at the Ahmadi Quarry. Figure 12, created using Petrel software, shows the general distribution and trends for fractures over the quarry area. These trends, which show a general N–S to NNE-SSW trend, have been used in guiding the modelling of fracture distribution patterns in a discrete fracture 3D model network. The fracture density might be a factor for porosity and permeability enhancement, being a corridor for gas leaks from the subsurface petroleum reservoir in this rich oil field. A hypothetical explanation and clarification follows.

5.1. Effect of hydrocarbon acidic gases on the porosity

The acidity of water increases when water penetrates soil with added organic acid (Mazzallo, 2004). Isotope studies by Khalaf et al. (2018) suggested that light carbon isotopes may have originated from the oxidation of upward escaping hydrocarbon gases along the dolostone fractures. The study area is located within the Greater Burgan oil field, which contains a large amount of hydrocarbon reservoirs in its Mesozoic rocks. The association of alunite within the dolocrete clastic fill is evidence supporting gas seepage (Khalaf and Abdullah, 2015). In fact, a study by Connan et al. (1999), on surface seepage in the Burgan Field, showed that a thin yellow film with a strong sulfuric smell and free crystalline native sulfur minerals was found at those locations. The results of their analyses for biomarkers in oil seepage show aerobic methanotrophic bacteria growing on the sour sulfur gas that permeates the surface.

Fractured and high-permeability rocks enhanced the penetration of acid water and accelerated the dissolution of the carbonate rocks (Figure 13-A). The Dammam Formation was uplifted by almost 400 m during the Oligocene period (Abdullah et al., 1997). This uplift caused some fracturing and exposed the area for almost 19 Ma (Figure 13-B), which enhanced meteoric water percolation and dissolution in the rocks. The pore meteoric water was able to dissolve the limestone and create extra pore spaces as vugs, moulds, or even caverns (Figure 4). According to Ehrenberg et al. (2012), much of the pore space in carbonate rocks is created at shallow depths. The alternative origin of secondary porosity is related to the acidic gases produced by the maturation processes of the kerogen in the source rocks, which can laterally and vertically migrate great distances and dissolve carbonate rock before oil migration occurs. Such complexity in the dissolution stages increases heterogeneity in porosity and permeability.

In Kuwait, acid gas generated from kerogen diagenesis began at 62 Ma (at the end of the Maastrichtian), predating the deposition of the Dammam Formation by approximately 15 Ma (Abdullah et al., 1997). Thus, these hydrocarbon acidic gases could have influenced the structure of the Dammam Formation at any time since its formation. The initial chertification along the bedding planes could account for a drop in the pH of sediments, causing silica precipitation. These acids, as well as the meteoric acidic water, dissolved parts of the karst dolostone after the Dammam uplift. The light δ^{13} C measured in these rocks by Khalaf et al. (2018) is suggested to have origins related to the oxidation of upwardly escaping hydrocarbon gases along fractures. The dissolution of mature dolocrete during the pluvial period was also likely enhanced by gas seepage during hydrocarbon formation. The sulfate-rich meteoric water may have led to the occurrence of hollow centred dolomite rhombs (Figure 6C-c). Gypsum precipitation within the calcitised dolocrete formed sulfate-rich solutions (Khalaf and Abdullah, 2015). The variation of silica material may cause fluctuations in silica concentrations and the pH of silcretisation solutions due to abundant meteoric water and acidic gas seepage (Leckie and Cheel, 1990). Abdullah and Connan (2002) found that oil migration from Kuwaiti source rocks occurred in pulses; this would have produced the acid gases in a similarly pulsating manner, which might have dissolved the previously cemented pores, adding further complexities to the diagenetic processes.

6. Conclusions

Although the studied section is only approximately 12 m thick, it shows that a tremendous amount of complicated diagenetic processes have had a great impact on both the porosity and permeability of the rock units.

The Dammam Formation was deposited in a tidal flat and back-lagoon environment and been subjected to many cycles of diagenesis, including dolomitisation, leaching, calcitisation, silicification, and dedolomitisation.

Porosity and permeability showed no clear trends within the 12 m layer, and the highest porosity and permeability occurred in the deepest unit of the studied chalky dolostone. The porosity and permeability in the lower and middle layers of the studied sections were higher than those in the topmost layers. Porosity varied laterally within each unit, making these rocks heterogeneous in both the horizontal and vertical directions. The highest average porosity (25 %) and permeability (1100 mD) were found in the chalky dolostone unit, while the lowest porosity (13 %) and permeability (130 mD) were found in the karst carapace unit.

The majority of the observed porosity is related to the leaching and fracturing processes in the rock framework, which is associated with rock exposure after uplifting, as well as acidic gas dissolution. Considering the porosity and permeability of the original rock in the depositional environment, most of the rocks have enhanced reservoir characteristics despite their complicated stages of cementation and recrystallisation.

Most of the porosity originated during the diagenesis processes, due to meteoric water dissolution. The dissolution of carbonate rocks can also be attributed to acidic gases, such as CO_2 and H_2S, formed during the thermal maturation of organic-rich source rock, or even from the oil in the reservoirs, which leaked through the fractures created when the Dammam was uplifted during or after the Oligocene period. Thus, the unconformities and fractures created in the carbonate rocks and acid gases from deeper formations have resulted in diagenetic process complexities, causing increased porosity and permeability in the studied rock. Therefore, the prediction of porosity and permeability in carbonate reservoirs along unconformities for petroleum exploration studies is challenging.

Although the Dammam Formation in the studied area is not an oil reservoir, the exposed rocks provide a great opportunity to visualise and quantify the variations in porosity and permeability that result from diagenesis associated with carbonate rocks along unconformities in a region rich in oil reservoirs, the Greater Burgan Field.

Declarations

Author contribution statement

Fowzia Abdullah: Conceived and designed the experiments; Performed the experiments; Analyzed and interpreted the data; Contributed reagents, materials, analysis tools or data; Wrote the paper.

Funding statement

This work was supported by a Kuwait University Research Grant (SE03/11).

Data availability statement

Data will be made available on request.

Declaration of interests statement

The authors declare no conflict of interest.

Additional information

No additional information is available for this paper.

Acknowledgements

The analytical services were provided by the Research Facility Unit at Kuwait University. The authors are grateful to the National Industrial Company in Kuwait and the management of the Al Ahmadi quarry for their continued support. Special thanks to Prof. Fikry Khalaf for his valuable comments and review of the manuscript. Acknowledgment is extended to Mr. Ismail Gharib, Mr. N. Bassili, and Mr. S. Chilwan for their assistance in the field and laboratory work. The author appreciates Ms. Sally Sayed for her help in drafting the figures. “Mr. Y. Abdullah, Mr. H. Mahmoud, and Ms. N. Al Motlak” are also acknowledged for their help in the preparation of thin sections and sample grinding from Kuwait University. Special thanks to Mr. Aimen Amer from Kuwait Schlumberger for constructing the 3D fracture model in Ahmadi Quarry.

References

Abdullah, F.H., Connan, J., 2002. Geochemical study of some Cretaceous rocks from Kuwait: comparison with oils from Cretaceous and Jurassic reservoirs. Org. Geochem. 33, 125–148.

Abdullah, F.H.A., Nederlof, P.J.R., Ormerod, M.P., Kinghorn, R., 1997. Thermal history of the lower and middle Cretaceous source rocks in Kuwait. GeoArabia 2, 151–164.

Aghli, Gh., Soleimani, B., Moussavi-Harami, R., Mohammadian, R., 2016. Fractured zones detection using conventional petrophysical logs by differentiation method and its correlation with image logs. J. Petrol. Sci. Eng. 142, 152–162.

Al-Awadi, E., Mukhopadhyay, A., Al-Senafy, M.N., 1999. Geology and hydrology of the Dammam Formation in Kuwait: Hydrology, 6, 302–314.

AL-Sulaimi, J.S., AL-Ruwaih, F.M., 2004. Geological, structural and geochemical aspects of the main aquifer systems in Kuwait. Kuwait Univ. J. Sci. Eng. 31, 149–174.

Alsharhan, A.S., Nairn, A.E.M., 1997. Sedimentary Basins and Petroleum Geology of the Middle East. Elsevier Science B.V., Amsterdam, The Netherlands, p. 942.

Bergstrom, R.E., Aten, R.E., 1964. Natural recharge and localization of fresh groundwater in Kuwait. J. Hydrol. 2, 213–231.

Beydoun, Z.R., 1988. The geological setting and tectonic framework of the Middle East. technical papers. In: Proceedings of the Seminar on Source and Habitat of Petroleum in the Middle East Arab Countries. Department of geology, American University of Beirut, Kuwait, pp. 5–72.

Buday, T., 1980. Stratigraphy and paleogeography. In: Kassab, I.M., Jassim, S.Z. (Eds.), The Regional Geology of Iraq, V. I: Stratigraphy and Paleogeography. State Organization for Minerals, Baghdad.

Burdon, D.J., Al-Sharhan, A., 1968. The problem of the paleokarstic Dammam limestone aquifer in Kuwait. J. Hydrol. 6, 385–404.

Carman, G.J., 1996. Structural elements of onshore Kuwait. GeoArabia 1, 239–266.

Connan, J., Lacrampe-Couloume, G., Adam, P., Albrecht, P., Abdullah, F.H., 1999. Unexpected organic geochemistry in the two famous oil/gas seepage of Kuwait: evidence of activity of methanotrophic bacteria at surface. In: 19th International Meeting on Organic Geochemistry, 6-10 September, Istanbul-Turkey, Abstract.

Dizaji, B.E., Bonab, H.R., 2009. Effect of depositional and diagenetic characteristics on carbonate reservoir quality: a case study from the South Pars gas field in the Persian Gulf. Petrol. Geosci. 15, 325–344.

Ehrenberg, S., Walderhaug, O., BjØrlykke, K., 2012. Carbonate porosity creation by mesogenetic dissolution: reality or illusion. Am. Assoc. Petrol. Geol. Bull. 96, 217–233.

Feazel, C., 2010. Using Modern Cave Systems as Analogs for Paleokarst Reservoirs: American Association Petroleum Geologists, Search and Discovery Article 50252. http://www.searchanddiscovery.com/documents/2010/50252feazel/ndx_feazel.pdf . (Accessed 25 April 2012).

Ford, D., Williams, P., 2007. Karst Hydrogeology and Geomorphology. John Wiley & Sons, Chichester, United Kingdom, p. 578.

Fuchs, W., Gattinger, T.E., Holzer, H.F., 1968. Explanatory Text to the Synoptic Geologic Map of Kuwait. Geological Survey of Austria, Vienna, p. 87.

Haq, B.U., Hardenbol, J., Vail, P.R., 1988. Mesozoic and Cenozoic chronostratigraphy and cycles of sea-level change. In: Wilgus, C.K., Hastings, B.S., Kendall, C.G. St.C., Posamentier, H., Van Wagoner, J., Ross, C.A. (Eds.), Sea-level Changes: an Integrated Approach: Society of Economic Paleontologists and Mineralogists, 42. Special Publication, pp. 71–108.

Hartmann, D.J., Beaumont, E.A., 1999. Predicting reservoir system quality and performance. In: Beaumont, E.A., Foster, N.H. (Eds.), Exploring for Oil and Gas Traps, Treatise of Petroleum Geology, Handbook of Petroleum Geology. American Association Petroleum Geologists distinguished publication chapter 9.

Khalaf, F.I., Abdullah, F.A., 2013. Petrography and diagenesis of cavity-fill dolocretes. Kuwait: Geoderma 207, 58–65.

Khalaf, F.I., Abdullah, F.A., 2015. Occurrence of diagenetic alunites within karst cavity infill of the Dammam Formation, Ahmadi, Kuwait: an indicator of hydrocarbon gas seeps. Arab. J. Geosci. 8, 1549–1556.

Khalaf, F., Mukhopadhyay, A., Naji, M., Sayed, M., Shublaq, W., Al-Otaibi, M., Hadi, K., Siwek, Z., Saleh, N., 1989. Geological assessment of the Eocene and post-eocene aquifers of Umm Gudair: Kuwait: Kuwait Inst. Sci. Res. Rep. (EES-91), KISR3176.

Khalaf, F.I., Abdullah, F.A., Gharib, I.M., 2018. Petrography, diagenesis and isotope geochemistry of dolostones and dolocretes in the Eocene Dammam Formation, Kuwait. Arab. Gulf: Carbonates Evaporites 33, 87–105.

Lababidi, M.M., Hamdan, A.N., 1985. Preliminary Lithostratigraphic Correlation Study in OAPEC Member Countries: Organization of Arab Petroleum Exporting Countries. Energy Resources Department, Kuwait, p. 171.

Leckie, D.A., Cheel, J.R., 1990. Nodular silcretes of the Cypress Hills formation (upper Eocene to middle Miocene) of southern saskatchewan, Canada. Sedimentology 37, 445–454.

Leyerer, K., Meyer, F., 2010. Burried Evaporite Paleokarsts in the Arab Evaporites and the Hith Formation, Saudi Arabia: Geo 2010 Middle East. Manama-Bahrain, Abstract.

Lindsay, R.F., Hughes, W., Aba Al-Hasan, S., 2010. Khuff-a Reservoir Porosity Creation and Destruction: A Product of Depositional and Diagenetic Processes, American Association Petroleum Geologists Annual Convention and Exhibition, 11-14 April 2010, Abstract.

Mahdi, T.A., Aqrawi, A.A., Horbury, A.D., Sherwani, G.H., 2013. Sedimentological characterization of the mid-Cretaceous Mishrif reservoir in southern Mesopotamian Basin, Iraq. Geoarabia 18 (1), 139–174.

Mazzallo, S.J., 2004. Overview of Porosity Evolution in Carbonate Reservoirs: American Association Petroleum Geologists Search and Discovery Article # 40134. http://www.kgslibrary.com/bulletins/bulletins.htm.

Mina, P., Razaghnia, M.T., Paran, Y., 1967. Geological and geophysical studies and exploratory drilling of the Iranian continental shelf. In: Proceedings Seventh World Petroleum Congress, 2. Elsevier, Barking, pp. 871–903.

Murray, R.C., 1960. Origin of porosity in carbonate rocks. J. Sediment. Petrol. 30, 59–84.

Owen, R.M., Nasr, S.W., 1958. Stratigraphy of the Kuwait–Basra area. In: Weeks, L.G. (Ed.), Habitat of Oil: America Association of Petroleum Geologists, Which Volume?, pp. 1252–1278.

Parson Corporation, 1963. Report to Government of Kuwait: Groundwater Resources of Kuwait, V. I. And II (Unpublished, personal contact).

Poros, Z., Mindszenty, A., Machel, H., Molnar, F., Ronchi, R., 2010. Powderization of Triassic dolostones in the Buda Hill, Hungary- an unusual type of karstification?. In: Advances in Carbonate Exploration and Reservoir Analysis: the Geological Society, London, 4-5 November, Book of Abstracts, pp. 66–68.

Sayago, J., Di Lucia, M., Mutti, M., Cotti, A., Sitta, A., Broberge, K., Przybylo, A., Buonaguro, R., Zimina, O., 2012. Characterization of a deeply buried paleokarst terrain in the Loppa High using core data and multiattribute seismic facies classification. Am. Assoc. Petrol. Geol. 96 (10), 1843–1866.

Schlanger, W., 2005. Carbonate Sedimentology and Sequence Stratigraphy. Society for Sedimentary Geology SEPM, Concepts in Sedimentology and Palaeontology Series No. 8, p. 200.

Selly, R.C., 1998. Elements of Petroleum Geology, second ed. Academic Press, London, p. 470p.

Swart, P.K., Cantrell, D.L., Westphal, H., Handford, C.R., Kendall, C.G., 2005. Origin of dolomite in the Arab-D reservoir from the Ghawar field, Saudi Arabia: evidence from petrographic and geochemical constraints. J. Sediment. Res. 75 (3), 476–491.

Tanoli, S.K., Al-Bloushi, J., 2017. Depositional History of the Eocene Dammam Formation in Kuwait: SPE-187628-MS, SPE Kuwait Oil & Gas Show and Conference, Kuwait, 15-18 October 2017.

Tucker, M.E., Wright, V.P., 1990. Carbonate Sedimentology. Balckwell, Oxford, p. 482.

Yamamoto, K., Al-Zinari, A., Ottinger, G., Edwards, E., Kompanil, G., Al-Ameri, M.B., 2011. Permeability characterizing of a high-K dolomitized interval: a case study from an Early Cretaceous carbonate reservoir of a giant Oil field. In: Offshore Abu Dhabi, United Arab Emirates: SPE Reservoir Characterisation and Simulation Conference and Exhibition, Abu Dhabi, UAE, 9-11 October, SPE 148254.

Ziegler, M.A., 2001. Late permian to Holocene paleofacies evolution of the Arabian Plate and its hydrocarbon occurrences. GeoArabia 6, 445–503.